This article has been accepted for publication in a future issue of this journal, but has not been fully edited. Content may change prior to final publication. Citation information: DOI 10.1109/TPWRS.2017.2705187, IEEE Transactions on Power Systems

Co-planning of Investments in Transmission and Merchant Energy Storage

Y. Dvorkin, *Student Member*, *IEEE*, R. Fernández-Blanco, Y. Wang, *Student Member*, *IEEE*, B. Xu, *Student Member*, *IEEE*, D. S. Kirschen, *Fellow*, *IEEE*, H. Pandžić, *Member*, *IEEE*, J.-P. Watson, *Member*, *IEEE*, and C. A. Silva-Monroy, *Member*, *IEEE*

***Abstract*—Suitably located energy storage systems are able to collect significant revenue through spatiotemporal arbitrage in congested transmission networks. However, transmission capacity expansion can significantly reduce or eliminate this source of revenue. Investment decisions by merchant storage operators must therefore account for the consequences of potential investments in transmission capacity by central planners. This paper presents a tri-level model to co-optimize merchant electrochemical storage siting and sizing with centralized transmission expansion planning. The upper level takes the merchant storage owner's perspective and aims to maximize the lifetime profits of the storage, while ensuring a given rate of return on investments. The middle level optimizes centralized decisions about transmission expansion. The lower level simulates market clearing. The proposed model is recast as a bi-level equivalent, which is solved using the column-and-constraint generation technique. A case study based on a 240-bus, 448-line testbed of the Western Electricity Coordinating Council interconnection demonstrates the usefulness of the proposed tri-level model.**

NOMENCLATURE

A. Sets and Indices

B	Set of buses, indexed by b.
E	Set of representative days, indexed by e.
I, I_b	Set of generating units and subset of generating units connected to bus b, indexed by i, $I_b \subseteq I$.
J	Set of iterations, indexed by j.
L, $\hat{L}$	Set of transmission lines and set of candidate lines for expansion, indexed by l, $\hat{L} \subseteq L$
T	Set of operating time intervals, indexed by t.
$\Omega_{[\cdot]}$	Set of decision variables for problem $[\cdot]$.
$o(l), r(l)$	Indices of the sending and receiving buses of line l.

B. Binary Variables

ω_l	Binary expansion decision on line l.

C. Parameters

C^{s}, C^{p}	Capital cost of storage per MWh (\$/MWh) and per MW (\$/MW) prorated on a daily basis.
$\hat{C}^{\mathrm{s}}$, $\hat{C}^{\mathrm{p}}$	Capital cost of storage per MWh (\$/MWh) and per MW (\$/MW).
C^{g}_i	Energy price offered by unit i, \$/MWh.
$C^{\mathrm{o}}_{etb}, C^{\mathrm{b}}_{etb}$	Offer and bid price of storage at bus b at interval t on day e, \$/MWh.
C^{u}_l	Capital cost of expansion for line l prorated on a daily basis, \$.
$\hat{C}^{\mathrm{u}}_l$	Capital cost of expansion for line l, \$.
D_{etb}	Demand at bus b at interval t on day e, MW.
$\overline{G}_i$	Maximum power output offered by unit i, MW.
G^0_{ei}	Initial power output of unit i on day e, MW.
$\overline{F}_l$, ΔF_l	Flow limit on transmission line l and its additional expansion capacity, MW.
$IC^{\max}$	Investment budget, \$.
N_B	Number of buses.
N_D	Number of days in a calendar year.
N_E	Number of representative days.
N_I	Number of generating units.
N_J	Number of iterations.
N_L	Number of transmission lines.
$N_{\hat{L}}$	Maximum number of candidate lines for expansion.
N_T	Number of time operating intervals.
R^{U}_i,R^{D}_i	Up and down ramp rate of unit i, MW/h.
RG^{f}_{etb}	Forecast offer quantity of renewable generation at bus b at interval t on day e, MW.
$x_l, \Delta x_l$	Reactance of line l and its expansion adjustment.
$\aleph^{\mathrm{c}}, \aleph^{\mathrm{d}}$	Charging/discharging efficiency of storage.
Λ	Energy storage lifetime.
Υ	Transmission line lifetime.
Ψ	Annual discount rate.
$\Delta\tau$	Duration of the operating interval t, h.
ρ	Energy-to-power ratio of energy storage, h.
π_e	Weight of day e.
χ	Rate of return on storage investments.
ε	Convergence tolerance.

D. Variables

$p^{\mathrm{b}}_{etb}, p^{\mathrm{o}}_{etb}$	Capacity bid (charging) and offer (discharging) of storage at bus b at interval t on day e, MW.
$\hat{p}^{\mathrm{c}}_{etb}, \hat{p}^{\mathrm{d}}_{etb}$	Storage charging and discharging injections at bus b at interval t on day e, MW.
s_{etb}	Storage state of charge at bus b at interval t on day e, MWh.
$\overline{s}_b$	Energy rating of storage at bus b, MWh.
f_{etl}	Power flow in line l at interval t on day e, MW.
g_{eti}	Power output of unit i at interval t on day e, MW.

This work was supported in part by the ARPA-E Green Electricity Network Integration (GENI) program under project DE-FOA-0000473, U.S. Department of Energy's National Nuclear Security Administration under Contract DE-AC04-94AL85000, as well as Croatian Science Foundation and Croatian TSO (HOPS) under project Smart Integration of RENewables - SIREN (I-2583-2015).

This article has been accepted for publication in a future issue of this journal, but has not been fully edited. Content may change prior to final publication. Citation information: DOI 10.1109/TPWRS.2017.2705187, IEEE Transactions on Power Systems

IC	Investment cost, \$.
P	Expected operating profit of storage, \$.
$\overline{p}_b$	Power rating of storage at bus b, MW.
SW_e,SW_e^{DLL}	Objective function of the primal and dual lower-level problems on day e, \$.
rs_{etb}	Renewable spillage at bus b at interval t on day e, MW.
θ_{etb}	Voltage phase angle at bus b at interval t on day e, rad.
η	Auxiliary variable.

I. Introduction

If current cost and performance trends continue, electrochemical storage will soon be widely deployed to perform spatiotemporal arbitrage and relieve transmission congestion [1]. However, transmission capacity expansion can significantly reduce or eliminate this source of revenue [2]. Investment decisions by merchant storage operators must therefore take into account the consequences of potential investments in transmission capacity by central planners. This paper proposes a framework for co-planning merchant electrochemical storage siting and sizing with centralized transmission expansion planning in systems with high renewable penetration levels.

A. Literature Review

While the joint generation and transmission capacity expansion has been studied previously [3]–[11], only some of these studies [6]–[12] model investments in energy storage. References [6]–[10] consider expansion in vertically-integrated utilities, where a single decision-maker is responsible for making all investment decisions. In [11], storage locations are optimized using the so-called 'arbitrage value' curves that are computed for all candidate locations based on locational marginal prices (LMPs). However, the approach in [11] does not explicitly maximize storage operating profits, as in [13], or endogenously ensure the full recovery of the investment cost, as in [12], [14]. To the best of the authors' knowledge, the joint storage and transmission expansion in a market environment has not been studied from a merchant storage perspective, i.e. when storage aims to maximize its lifetime profits and to recover fully the investment cost. Ignoring the merchant storage perspective in the joint storage and transmission planning produces expansion plans that hamper profitability of merchant investments. Related literature can be organized in the following three thrusts:

1) Storage siting and sizing: How to jointly optimize the siting and sizing of energy storage has been studied in a vertically-integrated context. The models presented in [10], [15]–[19] formulate this problem as a multi-stage mixed-integer linear program (MILP). These formulations minimize the sum of the operating and investment cost, thus balancing the short-term operational benefits against the long-term investment cost. In these models, energy storage investments are economically justified as long as the capital cost of an incremental addition of storage capacity is outweighed by the operating savings it produces. As pointed out in [15]–[17], [19], these decisions are sensitive to the penetration levels of renewable generation and the severity of network constraints, which can have a significant effect on the value of storage. While references [15]–[19] aim to reduce the operating cost, they do not explicitly account for the profitability of energy storage. For example, numerical simulations in [15] demonstrate that while achieving sizable system-wide operating cost savings, storage devices would not be able to collect enough profit to recover their investment cost if they were merchant. On the other hand, investors in merchant storage aim to maximize their profits and achieve a sufficient rate of return. Siting and sizing of merchant energy storage depends on sufficient profit opportunities [14], which are driven by the intra-day and inter-day LMP dynamics, which in turn depend on net nodal injections and the configuration of the transmission network [20]–[22]. Merchant storage should therefore be expected to act strategically in electricity markets to maximize its profit. Nasrolahpour *et al.* [23] propose a bi-level investment model to optimize storage sizing in a market environment. However, this model is tested on a single-bus representation of the Alberta electricity market, thus ignoring the effects of the transmission network on the profitability of storage investments [14].

2) Transmission expansion: For a number of reasons, including reliability concerns and regulatory uncertainty, transmission expansion planning has remained centralized in deregulated systems [4]. Munoz *et al.* [5] survey recent transmission expansion studies and propose a two-stage stochastic MILP for centralized transmission planning that derives an optimal transmission expansion plan. This model is tested on a 240-bus model of the Western Electricity Coordinating Council (WECC) system. Numerical results suggest that the most valuable investments involve reinforcing backbone transmission lines, i.e. capacity additions to existing corridors. Siting and sizing of merchant storage is particularly sensitive to backbone expansions because they can diminish or completely eliminate spatiotemporal arbitrage opportunities. De la Torre *et al.* [24] propose an MILP model to optimize transmission expansion decisions in a pool-based electricity market. This optimization is driven by both social welfare maximization and expansion cost minimization. In [25], the authors propose a bi-level model to optimize the transmission reinforcement decisions required to integrate wind generation in a market environment. None of references [4], [5], [24], [25] consider the effect of storage on transmission investments.

3) Storage and transmission co-planning: Since energy storage can relieve congestion in the transmission network, co-planning of energy storage and transmission expansion can increase their overall value to the system. Co-planning has been investigated in a vertically-integrated context [6]–[10]. These authors propose single-level MILPs with multi-stage decision making that aims to co-optimize the investment and operating costs and show that co-optimized energy storage and transmission decisions lead to more cost savings, more efficient congestion relief, and an increased utilization of renewable generation than when these decisions are optimized separately. Qi *et al.* [6] emphasize that even small-sized distributed energy storage yields significant benefits, but remark that the incremental value of energy storage diminishes faster than that of transmission lines. In line with [6], Konstantelos

This article has been accepted for publication in a future issue of this journal, but has not been fully edited. Content may change prior to final publication. Citation information: DOI 10.1109/TPWRS.2017.2705187, IEEE Transactions on Power Systems

et al. [7] demonstrate that energy storage, as well as other non-conventional generation assets, provides extra value in systems with renewables and stringent inter-temporal and N-1 security constraints. However, the trade-off between energy storage and transmission expansion decisions in the presence of uncertain generation, e.g. [26], [27], is not always straightforward. For example, Qiu *et al.* [8] conclude that transmission planning tends to affect optimal energy storage locations, but does not noticeably change the total installed capacity. Similarly, Hedayati *et al.* [9] demonstrate that storage provides most value when located in congested areas and co-optimized with transmission expansion. Go *et al.* [10] propose a model to co-optimize investments in generation, transmission, and energy storage assets and conclude that storage investments are likely to defer and reduce investments in other assets.

A common characteristic of [3], [4], [6]–[10], [15]–[17], [20], [24], [25] is that their case studies are carried out on various modifications of the IEEE Reliability Test System. Numerical conclusions in [19] and [23] are derived on a simplified representation of realistic systems with one or several buses. Unlike in [3], [4], [6]–[10], [16], [17], [19], [20], [23]–[25], case studies in [5], [15] and [18] are performed on reasonably realistic, large-scale modifications of the WECC (240 buses) and the BPA (2209 buses) systems, which offer both realistic qualitative and quantitative insights.

B. Contributions

This paper addresses the issue of merchant storage siting and sizing in a market environment with centralized transmission planning. It makes the following contributions:

1) This paper presents a new tri-level (TL) model that optimizes merchant storage siting and sizing decisions and centralized transmission expansion decisions. The lifetime profit of storage is expressed as an explicit function of LMPs and storage charging and discharging decisions. The expected lifetime profit collected by storage is related to the investment cost of storage in order to enforce a desired rate of return on investments.
2) The proposed TL model is tested on a realistically large 240-bus WECC system. These tests illustrate the optimal trade-off between merchant storage siting and sizing and transmission expansion decisions under different operational conditions and investment scenarios.

This TL model should be useful to regulators, system planners, and investors in techno-economic analyses of storage investments as well as understanding interactions between storage and transmission expansion decisions.

II. Formulation

Fig. 1 illustrates the structure and shows the interfaces between the different levels of the proposed TL optimization. The upper-level (UL) problem implements the merchant storage perspective, i.e. it minimizes the investment cost and maximizes the expected profit of storage. The UL problem submits the optimal storage capacity bids (p^{b}_{etb}) and offers (p^{o}_{etb}) to the system operator (SO), which is represented in the lower-level (LL) problems. The UL problem also ensures that the expected operating profit of merchant storage computed based on the LMPs (λ_{etb}) produced by the LL problems is sufficient to recover the investment cost. The middle-level (ML) problem takes the perspective of the SO and minimizes the system-wide operating cost and the cost of centralized transmission expansion. The expansion decisions, ω_l, made by the ML problem are enforced in the LL problem. The LL problems implement the day-ahead market-clearing mechanisms [28] performed by the SO. These problems maximize the social welfare given the decisions made by the UL and ML problems. The TL optimization is carried out over a set of representative days capturing various operating conditions.

A. Assumptions

In this paper we make a set of assumptions that are similar to those made in previous publications [3]–[9], [14]–[20], [23]–[25], [29]:

1) The investment decisions in the UL and ML problems are optimized for a single target year.
2) The UL problem takes a viewpoint of the single energy storage merchant. Multiple storage merchants can be considered using an equilibrium problem with equilibrium constraints (EPEC) framework [30].
3) The UL problem assumes that merchant storage has knowledge of potential transmission expansion decisions considered by the SO. In practice, this information can be learned from public hearings organized by the SO or planning authority [31].
4) The ML problem optimizes transmission expansion decisions in a centralized manner [4].
5) Since construction of new lines extends beyond the expected lifetime (10-15 years) of most battery storage technologies [29], the transmission expansion decisions are limited to backbone upgrades [5].
6) The transmission network is represented using a lossless dc power flow model.
7) We assume perfect competition and hourly time intervals in the day-ahead market [28]. Pricing is done on a nodal and hourly basis, i.e. producers and consumers get

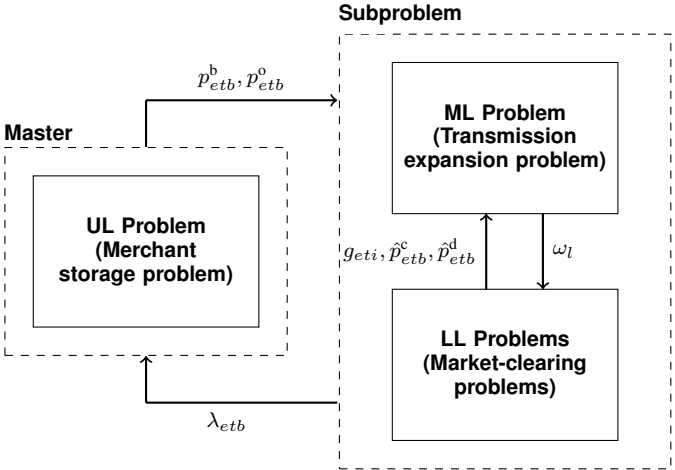

Fig. 1. Structure of the proposed TL model. The decomposition into the master and subproblem follows the implementation described in Section III-C.

This article has been accepted for publication in a future issue of this journal, but has not been fully edited. Content may change prior to final publication. Citation information: DOI 10.1109/TPWRS.2017.2705187, IEEE Transactions on Power Systems

paid and pay the LMP calculated at the bus where they are located [28]. Hence, our analyses do not consider real-time price fluctuations that can increase storage profitability.

8) Merchant storage optimizes its bids and offers to maximize its profits. Other market participants bid and offer at their marginal utility and cost.
9) Demand is inelastic [5] and representative demand profiles are deemed to capture a future demand growth and internalize flexibility of controllable loads [32].
10) To avoid dealing with non-convex prices and to reduce the computation burden, the minimum up- and down-times, binary on/off statuses, and minimum power outputs of conventional generators are ignored in the LL problems, as in [17], [18], [23], [25], [32]. This assumption makes conventional generators more flexible than in practice. However, it is expected that systems with large renewable penetrations will require more flexible conventional generation [33], [34]. This assumption may therefore underestimate the operational benefits of transmission expansion decisions for current systems. On the other hand, competing with very flexible generators is a worst-case scenario from the perspective of a storage owner. Therefore, this assumption yields conservative decisions about merchant storage investments.

B. Upper-Level Problem

$$\max_{\Omega_{\text{UL}}} \quad P - IC \tag{1}$$

Subject to:

$$P := \sum_{e\in E}\pi_e \sum_{b\in B}\sum_{t\in T}\left((\lambda_{etb}-C^{\text{o}}_{etb})p^{\text{o}}_{etb}-(\lambda_{etb}-C^{\text{b}}_{etb})p^{\text{b}}_{etb}\right) \tag{2}$$

$$IC := \sum_{b\in B}\left(C^{\text{s}}\overline{s}_b + C^{\text{p}}\overline{p}_b\right) \le IC^{\max} \tag{3}$$

$$P \ge \chi \cdot IC \tag{4}$$

$$\overline{p}_b = \overline{s}_b/\rho, \forall b \in B \tag{5}$$

$$s_{etb} = s_{e,t-1,b} + (p^{\text{b}}_{etb}\aleph^{\text{c}} - p^{\text{o}}_{etb}/\aleph^{\text{d}})\Delta\tau, \quad \forall e\in E, t\in T, b\in B \tag{6}$$

$$0 \le p^{\text{b}}_{etb}\aleph^{\text{c}} \le \overline{p}_b, \forall e\in E, t\in T, b\in B \tag{7}$$

$$0 \le p^{\text{o}}_{etb}/\aleph^{\text{d}} \le \overline{p}_b, \forall e\in E, t\in T, b\in B \tag{8}$$

$$0 \le s_{etb} \le \overline{s}_b, \forall e\in E, t\in T, b\in B, \tag{9}$$

where $\Omega_{\text{UL}} = \left\{IC, p^{\text{b}}_{etb}, p^{\text{o}}_{etb}, P, \overline{p}_b, s_{etb}, \overline{s}_b\right\}$. The objective function (1) maximizes the difference between the expected operating profit of storage over representative days and the investment cost. This expected operating profit is computed in (2) based on the revenue collected in the market and the discharging and charging operating costs, as modeled in [17]. The dual variable λ_{etb} is associated with the power balance constraint of the LL problems (22). The investment cost is computed in (3), where parameters C^{s} and C^{p} are the daily prorated costs in the net present value approach, [16]:

$$C^{\text{s}} = \hat{C}^{\text{s}}\frac{\Psi(1+\Psi)^{\Lambda}}{(1+\Psi)^{\Lambda}-1}\cdot\frac{1}{N_{\text{D}}} \tag{10}$$

$$C^{\text{p}} = \hat{C}^{\text{p}}\frac{\Psi(1+\Psi)^{\Lambda}}{(1+\Psi)^{\Lambda}-1}\cdot\frac{1}{N_{\text{D}}}. \tag{11}$$

Parameters $\hat{C}^{\text{s}}$ and $\hat{C}^{\text{p}}$ are the energy- and power-related components of the energy storage investment cost, Ψ is the annual discount rate, Λ is the energy storage lifetime, and N_{D} is the number of days in the target year. Constraint (4) relates the expected profit and the investment cost via parameter $\chi \ge 1$, thus enforcing a desired rate of return. Constraint (5) relates the energy and power ratings of storage using a technology-specific parameter ρ. Constraints (6)–(9) limit the operation of storage to its nameplate power and energy ratings[1].

C. Middle-Level Problem

$$\min_{\Omega_{\text{ML}}} \sum_{l\in\hat{L}} C^{\text{u}}_l\omega_l + \sum_{e\in E}\pi_e\sum_{t\in T}\Big(\sum_{i\in I}C^{\text{g}}_i g_{eti} + \sum_{b\in B}\left(C^{\text{o}}_{etb}\hat{p}^{\text{d}}_{etb} - C^{\text{b}}_{etb}\hat{p}^{\text{c}}_{etb}\right)\Big) \tag{12}$$

Subject to:

$$\sum_{l\in\hat{L}}\omega_l \le N_{\hat{L}} \tag{13}$$

$$\omega_l \in \{0,1\}, \forall l \in \hat{L} \tag{14}$$

$$\omega_l = 0, \forall l \notin \hat{L}, \tag{15}$$

where $\Omega_{\text{ML}} = \left\{\omega_l\right\}$. The objective function (12) minimizes the cost of the transmission expansion decisions and the expected system operating cost over representative days. Similarly to (10)–(11), parameter C^{u}_l is computed using the net present value approach [16]:

$$C^{\text{u}}_l = \hat{C}^{\text{u}}_l\frac{\Psi(1+\Psi)^{\Upsilon}}{(1+\Psi)^{\Upsilon}-1}\cdot\frac{1}{N_{\text{D}}}. \tag{16}$$

Parameter C^{u}_l is the capital cost of expansion for transmission line l and Υ is the transmission line lifetime. Constraint (13) limits the number of binary transmission expansion decisions ω_l declared in (14) and (15). Donohoo [29] has shown that the cardinality of $\hat{L}$ is usually small. This constraint limits the number of binary variables in the ML problem and makes it computational tractable. LL variables g_{eti}, $\hat{p}^{c}_{etb}$, and $\hat{p}^{d}_{etb}$ are parametrized in the ML problem.

D. Lower-Level Problem

For each representative day e, the LL problem is as follows:

$$\max_{\Omega_{\text{LL}}} SW_e := -\sum_{t\in T}\sum_{i\in I}C^{\text{g}}_i g_{eti} - \sum_{t\in T}\sum_{b\in B}\left(C^{\text{o}}_{etb}\hat{p}^{\text{d}}_{etb} - C^{\text{b}}_{etb}\hat{p}^{\text{c}}_{etb}\right) \tag{17}$$

Subject to:

$$0 \le g_{eti} \le \overline{G}_i : (\overline{\alpha}_{eti}), \forall i\in I, t\in T \tag{18}$$

[1]To prevent simultaneous charging and discharging of stored energy, constraints (7)–(8) can be modified as $0 \le p^{\text{b}}_{etb}\aleph^{\text{c}} \le \overline{p}_b a_{etb}$ and $0 \le p^{\text{o}}_{etb}/\aleph^{\text{d}} \le \overline{p}_b(1-a_{etb})$, where $a_{etb} \in \{0,1\}$ [10], [35].

This article has been accepted for publication in a future issue of this journal, but has not been fully edited. Content may change prior to final publication. Citation information: DOI 10.1109/TPWRS.2017.2705187, IEEE Transactions on Power Systems

$$-RD_i \le g_{eti} - g_{e,t-1,i} \le RU_i : (\underline{\beta}_{eti}, \overline{\beta}_{eti}), \quad \forall i \in I, t \in T \tag{19}$$

$$f_{etl}(x_l - \omega_l \Delta x_l) = \theta_{et,o(l)} - \theta_{et,r(l)} : (\xi_{etl}), \quad \forall l \in L, t \in T \tag{20}$$

$$-\overline{F}_l - \omega_l \Delta F_l \le f_{etl} \le \overline{F}_l + \omega_l \Delta F_l : (\underline{\delta}_{etl}, \overline{\delta}_{etl}), \quad \forall l \in L, t \in T \tag{21}$$

$$D_{etb} = \sum_{i \in I_b} g_{eti} - \sum_{l|o(l)=b} f_{etl} + \sum_{l|r(l)=b} f_{etl} + \big(RG^{\mathrm{f}}_{etb} - rs_{etb}\big) - \hat{p}^{\mathrm{c}}_{etb} + \hat{p}^{\mathrm{d}}_{etb} : (\lambda_{etb}), \forall b \in B, t \in T \tag{22}$$

$$0 \le rs_{etb} \le RG^{\mathrm{f}}_{etb} : (\gamma_{etb}), \forall b \in B, t \in T \tag{23}$$

$$0 \le \hat{p}^{\mathrm{c}}_{etb} \le p^{\mathrm{b}}_{etb} : (\phi^{\mathrm{c}}_{etb}), \forall b \in B, t \in T \tag{24}$$

$$0 \le \hat{p}^{\mathrm{d}}_{etb} \le p^{\mathrm{o}}_{etb} : (\phi^{\mathrm{d}}_{etb}), \forall b \in B, t \in T, \tag{25}$$

where $\Omega_{\mathrm{LL}} = \big\{f_{etl}, g_{eti}, \hat{p}^{\mathrm{c}}_{etb}, \hat{p}^{\mathrm{d}}_{etb}, rs_{etb}, \theta_{etb}\big\}$. The objective function (17) maximizes the social welfare, which is defined based on the assumptions in Section II-A as minus the sum of the cost of the accepted generation offers and of the cost of the accepted ES offers and bids. Constraints (18) enforce the maximum limit on the capacity offers of conventional generators. The upward/downward ramp rate limits of conventional generators are constrained in (19). Constraints (20) and (21) compute the power flows and enforce the transmission limits. If ω_l is set to 1 by the ML problem, constraints (20) and (21) account for the equivalent reactance ($x_l - \Delta x_l$) and power flow limit ($\overline{F}_l + \Delta F_l$) of the upgraded line. Constraint (22) models the nodal power balance, where renewable spillage is limited by (23) and storage charging and discharging injections are limited in (24)–(25) by the bids and offers optimized in the UL problem. The dual variables of the LL constraints are specified behind a colon in (18)–(25).

III. Solution Technique

To solve the TL problem, the ML and LL problems are first converted into a single-level equivalent using the duality-based approach [36], [37]. This approach consists in replacing the convex LL problem by its primal and dual feasibility constraints and the strong duality equality so that a single-level equivalent of the ML and LL problems is obtained. This transforms the original TL problem into the equivalent bi-level (BL) problem described in Section III-B. This BL problem is then solved using the column-and-constraint generation (CCG) algorithm [38], as explained in Section III-C.

A. Dual Lower-Level Problem

Since the LL problem is convex, the dual LL (DLL) problem for each representative day e is:

$$\min_{\Omega_{\mathrm{DLL}}} SW^{\mathrm{DLL}}_e := \sum_{t \in T} \sum_{i \in I} \big(\overline{\alpha}_{eti} \overline{G}_i + \overline{\beta}_{eti} RU_i - \underline{\beta}_{eti} RD_i\big) + \sum_{i \in I} \big(\overline{\beta}_{e1i} + \underline{\beta}_{e1i}\big) G^0_{ei} + \sum_{t \in T} \sum_{b \in B} \Big(\gamma_{etb} RG^{\mathrm{f}}_{etb} + \phi^{\mathrm{c}}_{etb} p^{\mathrm{b}}_{etb} + \phi^{\mathrm{d}}_{etb} p^{\mathrm{o}}_{etb} + \lambda_{etb}(D_{etb} - RG^{\mathrm{f}}_{etb})\Big) + \sum_{t \in T} \sum_{l \in L} (\overline{\delta}_{etl} - \underline{\delta}_{etl}) \times (\overline{F}_l + \omega_l \Delta F_l) \tag{26}$$

Subject to:

$$-\sum_{l|o(l)=b} \xi_{etl} + \sum_{l|r(l)=b} \xi_{etl} = 0, \forall b \in B, t \in T \tag{27}$$

$$\xi_{etl}(x_l - \omega_l \Delta x_l) + \overline{\delta}_{etl} + \underline{\delta}_{etl} - \lambda_{et,o(l)} + \lambda_{et,r(l)} = 0, \quad \forall l \in L, t \in T \tag{28}$$

$$\gamma_{etb} - \lambda_{etb} \ge 0, \forall b \in B, t \in T \tag{29}$$

$$\overline{\alpha}_{eti} + \overline{\beta}_{eti} - \overline{\beta}_{e,t+1,i} + \underline{\beta}_{eti} - \underline{\beta}_{e,t+1,i} + \lambda_{et,b(i)} \ge -C^{\mathrm{g}}_i, \forall t = 1...N_T - 1, i \in I \tag{30}$$

$$\overline{\alpha}_{eti} + \overline{\beta}_{eti} + \underline{\beta}_{eti} + \lambda_{et,b(i)} \ge -C^{\mathrm{g}}_i, \forall t = N_T, i \in I \tag{31}$$

$$\phi^{\mathrm{c}}_{etb} - \lambda_{etb} \Delta\tau \ge C^{\mathrm{b}}_{etb}, \forall b \in B, t \in T \tag{32}$$

$$\phi^{\mathrm{d}}_{etb} + \lambda_{etb} \Delta\tau \ge -C^{\mathrm{o}}_{etb}, \forall b \in B, t \in T \tag{33}$$

$$\overline{\alpha}_{eti}, \overline{\beta}_{eti}, \gamma_{etb}, \overline{\delta}_{etl}, \phi^{\mathrm{c}}_{etb}, \phi^{\mathrm{d}}_{etb} \ge 0, \underline{\beta}_{eti}, \underline{\delta}_{etl} \le 0, \tag{34}$$

where $\Omega_{\mathrm{DLL}} = \big\{\overline{\alpha}_{eti}, \overline{\beta}_{eti}, \gamma_{etb}, \overline{\delta}_{etl}, \phi^{\mathrm{c}}_{etb}, \phi^{\mathrm{d}}_{etb}, \underline{\beta}_{eti}, \underline{\delta}_{etl}, \xi_{etl}, \lambda_{etb}\big\}$. Note that constraint (34) restricts the domain of dual variables.

B. Equivalent Bi-Level Model

Using the DLL constraints (27)–(34) and applying the strong duality theorem [36], the original TL problem is converted into the following BL equivalent:

$$\max_{\Omega_{\mathrm{UL}}} \quad P - IC \tag{35}$$

Subject to:

$$\text{Equations (2)–(9)} \tag{36}$$

$$\lambda_{etb} \in \underset{\Omega_{\mathrm{ML}} \cup \Omega_{\mathrm{LL}} \cup \Omega_{\mathrm{DLL}}}{\arg\min} \Big\{ \sum_{l \in \hat{L}} C^{\mathrm{u}}_l \omega_l + \sum_{e \in E} \pi_e \sum_{t \in T} \Big(\sum_{i \in I} C^{\mathrm{g}}_i g_{eti} + \sum_{b \in B} \big(C^{\mathrm{o}}_{etb} \hat{p}^{\mathrm{d}}_{etb} - C^{\mathrm{b}}_{etb} \hat{p}^{\mathrm{c}}_{etb}\big)\Big) \tag{37}$$

Subject to:

$$\text{Equations (13)–(15)}, \big\{\text{Equations (18)–(25), (27)–(34)}, \forall e \in E\big\}, \tag{38}$$

$$SW_e = SW^{\mathrm{DLL}}_e, \forall e \in E\Big\}, \tag{39}$$

where (36) represents the constraints of the UL problem and (37)–(39) are the single-level equivalent of the ML and LL problems. As in the duality-based approach described in [36], (38) includes the ML, LL, and DLL constraints and (39) enforces the strong duality condition. The optimization in (37)–(39) is performed over $\Omega_{\mathrm{ML}} \cup \Omega_{\mathrm{LL}} \cup \Omega_{\mathrm{DLL}}$, i.e. the ML, LL, and DLL variables are co-optimized.

The single-level equivalent of the ML and LL problems (37)–(39) is nonlinear due to the terms $f_{etl}\omega_l\Delta x_l$ in (20), $\overline{\delta}_{etl}\omega_l\Delta F_l$ and $\underline{\delta}_{etl}\omega_l\Delta F_l$ in (26), $\xi_{etl}\omega_l\Delta x_l$ in (28) because they involve the product of continuous and binary variables. Such products can be linearized using the 'Big M' method [39], thus converting (37)–(39) into an MILP.

C. CCG Algorithm

The BL equivalent described in (35)–(39) is decomposed into a master and subproblem and solved using the CCG algorithm illustrated in Fig. 2. As demonstrated via numerical

This article has been accepted for publication in a future issue of this journal, but has not been fully edited. Content may change prior to final publication. Citation information: DOI 10.1109/TPWRS.2017.2705187, IEEE Transactions on Power Systems

simulations in [38], the computational performance of the CCG algorithm is generally better than Benders' decomposition, which has also been used in planning studies [40], [41]. This is achieved by using primal cuts instead of dual cuts. Interested readers are referred to [38] for a full description of the CCG algorithm, including convergence and other algorithmic properties, and to [32] for its application in transmission expansion studies. Each step of the CCG algorithm implemented in this study is described below:

- **Step 0:** The upper (UB) and lower bounds (LB) are set to ∞ and $-\infty$ and the iteration counter is set to $j = 0$. The initial values of the LMPs, $\lambda_{etb}^{(j=0)}$, are set to the LMPs for the case without added transmission and storage, i.e. $\omega_l^{(j=0)} = 0$, $\overline{e}_b^{(j=0)} = 0$, $\overline{p}_b^{(j=0)} = 0$.
- **Step 1:** Update the iteration counter, i.e. $j \leftarrow j + 1$.
- **Step 2:** Solve the following master problem (MP):

$$\max_{\Omega_{\text{UL}}} \sum_{e\in E}\pi_e \sum_{b\in B}\sum_{t\in T}\lambda_{etb}^{(j)}\left(p_{etb}^{\text{o},(j)} - p_{etb}^{\text{b},(j)}\right) - \eta - IC^{(j)} \quad (40)$$

Subject to:

$$\text{Equations (3)–(9)} \quad (41)$$

$$\eta \geq \sum_{e\in E}\pi_e \sum_{t\in T}\sum_{b\in B}\left(C_{etb}^{\text{o}}\hat{p}_{etb}^{\text{d},(k)} - C_{etb}^{\text{b}}\hat{p}_{etb}^{\text{c},(k)}\right), \forall k \leq j \quad (42)$$

$$\hat{p}_{etb}^{\text{c},(k)} \leq p_{etb}^{\text{b},(k)}, \forall e \in E, t \in T, b \in B, 1 < k \leq j \quad (43)$$

$$\hat{p}_{etb}^{\text{d},(k)} \leq p_{etb}^{\text{o},(k)}, \forall e \in E, t \in T, b \in B, 1 < k \leq j. \quad (44)$$

The UL constraints are included in (41). Constraints (42)–(44) are the cuts added to the master at every iteration of the CCG algorithm. Note that cuts in (42)–(44) are only added for iterations $j > 1$ since they require the SP solution. In order to avoid infeasibilities in the MP, we limit the column generation to the previous iteration, i.e. $k = j - 1$. Once the MP is solved, recalculate $LB = \sum_{e\in E}\pi_e \sum_{t\in T}\sum_{b\in B}(C_{etb}^{\text{o}} p_{etb}^{\text{o},(j)} - C_{etb}^{\text{b}} p_{etb}^{\text{b},(j)})$.

- **Step 3:** The following subproblem (SP) is solved:

$$\min_{\Omega_{\text{ML}}\cup\Omega_{\text{LL}}\cup\Omega_{\text{DLL}}} \sum_{l\in\hat{L}} C_l^{\text{u}}\omega_l^{(j)} + \sum_{e\in E}\pi_e \sum_{t\in T}\Big(\sum_{i\in I} C_i^{\text{g}} g_{eti}^{(j)} + \sum_{b\in B}\left(C_{etb}^{\text{o}}\hat{p}_{etb}^{\text{d},(j)} - C_{etb}^{\text{b}}\hat{p}_{etb}^{\text{c},(j)}\right)\Big) \quad (45)$$

Subject to:

$$\text{Constraints (13)–(15)} \quad (46)$$

$$\text{Constraints (18)–(23), (27)–(34), (39)}, \forall e \in E \quad (47)$$

$$0 \leq \hat{p}_{etb}^{\text{c},(j)} \leq p_{etb}^{\text{b},(j)}, \forall b \in B, e \in E, t \in T \quad (48)$$

$$0 \leq \hat{p}_{etb}^{\text{d},(j)} \leq p_{etb}^{\text{o},(j)}, \forall b \in B, e \in E, t \in T. \quad (49)$$

The ML constraints are included in (46). The LL and DLL constraints, as well as the strong duality condition, are given in (47). Note that constraints (24)–(25) in the original LL problem are replaced with constraints (48)–(49) in the SP problem, where $p_{etb}^{\text{b},(j)}$ and $p_{etb}^{\text{o},(j)}$ are the MP solution at iteration j. Once the SP is solved, recalculate $UB = \sum_{e\in E}\pi_e \sum_{t\in T}\sum_{b\in B}(C_{etb}^{\text{o}}\hat{p}_{etb}^{\text{d},(j)} - C_{etb}^{\text{b}}\hat{p}_{etb}^{\text{c},(j)})$.

- **Step 4:** If $|UB - LB|/UB < \varepsilon$, the algorithm stops. Otherwise, go to step 1.

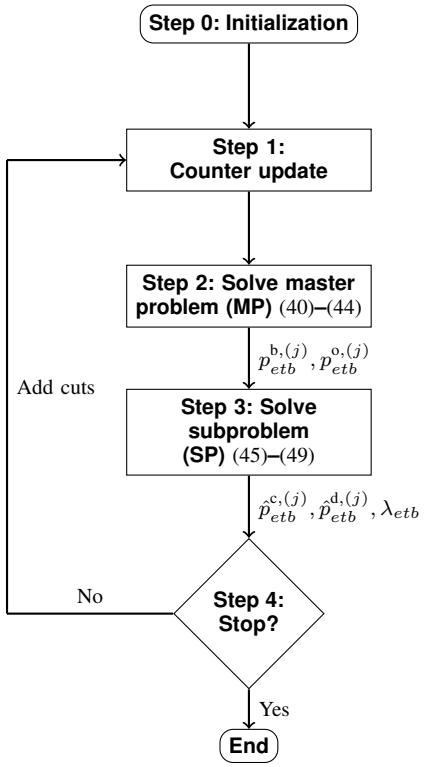

Fig. 2. Flowchart of the CCG algorithm used to solve the BL equivalent shown in Section III-B. Each step is further detailed in Section III-C.

D. Computational Complexity

Solving the proposed TL model with the CCG algorithm requires solving the linear MP and mixed-integer linear SP at each iteration. The number of constraints and decision variables in the MP and SP are given in Table I. As more cuts are added at every iteration of the CCG algorithm, the number of constraints and continuous decision variables in the MP increases moderately. On the other hand, the complexity of the SP arises from the need to account for $N_{\hat{L}}$ binary variables for line expansion decisions and the need to consider N_E representative days. Hence, carefully pre-selecting candidate lines for expansion decisions and the use of advanced scenario reduction techniques to choose the least-possible number of representative days will reduce the computational complexity of the SP.

TABLE I. DIMENSION OF THE MASTER PROBLEM (MP) AND SUBPROBLEM (SP) PER ITERATION

	# constraints	# continuous variables	# binary variables
MP, $j = 1$	$3 + N_B(1 + 4N_T N_E)$	$1 + N_B(2 + 3N_T N_E)$	–
MP, $j > 1$	$3 + N_B(1 + 6N_T N_E) + N_j$	$N_B(2 + 3N_T N_E)$	–
SP	$2 + N_L - N_{\hat{L}} + N_T N_E(8N_B + 4N_I + 4N_L)$	$N_T N_E(8N_B + 4N_I + 4N_L)$	$N_{\hat{L}}$

IV. WECC CASE STUDY

A. Data and Experimental Setup

The proposed TL model is solved on a 240-bus, 448-line model of the WECC interconnection [42] with the con-

This article has been accepted for publication in a future issue of this journal, but has not been fully edited. Content may change prior to final publication. Citation information: DOI 10.1109/TPWRS.2017.2705187, IEEE Transactions on Power Systems

ventional and renewable generation portfolios anticipated by 2024 as described in the 2024 WECC PC1 Common Case report [43]. The conventional generation mix includes 50 gas-fired (77.8 GW), 27 hydro (66.8 GW), 17 coal-fired (32.6 GW), and 4 nuclear (9.8 GW) power plants. The renewable generation portfolio consists of 32 wind (24.7 GW), 7 solar (8.8 GW), 6 geothermal (2.5 GW), and 3 biomass (0.6 GW) power plants, as well as 11 generic renewable (1.9 GW) power plants. The hourly average system-wide peak and valley loads are 141.5 GW and 68 GW throughout the target year. Renewable generation is assumed to be controllable and spillage is allowed at no cost. The annual load and renewable generation profiles were reduced to 5 representative daily profiles, each with 24 hourly operating intervals, using the hierarchical clustering algorithm described in [44]. This algorithm performs a general-to-specific partitioning, which recursively distributes daily profiles at every bus among a given number of clusters based on their similarity. Alternative clustering algorithms [45]–[47] can be used instead, as well as the number of representative days can be increased to improve the accuracy of the results at expense of a higher computational cost.

The planning horizon for storage expansion is assumed to be 10 years. Prospective battery storage technologies are represented by a generic battery model with symmetric charging and discharging efficiencies $\aleph^{\mathrm{c}} = \aleph^{\mathrm{d}} = 0.9$ and energy-to-power ratio $\rho = 5$ h; these parameters are feasible for performing spatiotemporal arbitrage [1], [14]–[16]. As in [14] and [16], the prospective capital cost of different storage technologies is accounted for using three capital cost scenarios: low ($20/kWh and $500/kW), medium ($50/kWh and $1,000/kW), and high ($75/kWh and $1,300/kW)[2]. Unless stipulated otherwise, $\chi = 1$, which ensures that all storage investments are exactly recovered [14], and the investment budget is unlimited, i.e. $IC^{\max} = \infty$. The price bids and offers of energy storage are $C^{\mathrm{b}}_{etb} = \$100$/MWh and $C^{\mathrm{o}}_{etb} = \$0$/MWh, which ensures that these bids and offers are always cleared in the electricity market [14], [21]. To simulate space constraints at each substation, the energy capacity of the storage that can be placed at each bus is limited to 200 MWh unless stipulated otherwise. The baseline cost of transmission expansion is assumed to be as in [49] and varies from $959,700/mi (230 kV) to $1,919,450/mi (500 kV), which includes the cost of substation upgrades and right-of-ways. Since the transmission expansion in this work assumes backbone upgrades only [5], the baseline costs are multiplied by a scaling factor ranging from 35% (230 kV) to 55% (500 kV) [49]. The storage and transmission expansion costs are prorated on a daily basis using the net present value approach, as explained in [16], with an annual interest rate of 5%. Similarly to [8], [14], [15], the lifetime of storage and transmission lines is assumed to be 10 and 60 years, respectively, with no residual worth.

All computations were carried out on the Hyak supercomputer system at the University of Washington [50], running CPLEX [51] under GAMS 23.7 [52] on an Intel Xenon 2.55 GHz processor with at least 32 GB of RAM. The convergence tolerance of the CCG approach is $\varepsilon = 0.3\%$ and the optimality gap was set to 0.1% for all simulations.

The following numerical analyses are performed for merchant energy storage providing spatiotemporal arbitrage in a day-ahead electricity market. Additional profit streams can be added to (2), e.g. from capacity, ancillary services, hour-ahead markets, but are beyond the scope of this paper. Simultaneous participation in multiple markets may increase merchant storage profitability.

B. Merchant Storage without Transmission Expansion

When no transmission expansion is considered, i.e. $N_{\hat{L}} = 0$, the TL model produces the storage siting and sizing decisions displayed in Fig. 3. Since the energy and power ratings of ES are assumed to be related by parameter ρ, all sizing decisions are described in terms of the energy ratings ($\overline{s}_b$). The siting decisions are predictably driven by the capital cost scenario and the number of locations increases as the capital cost reduces. Under the high capital cost scenario, storage is installed at bus #155 only, which is also the only common bus for all three capital cost scenarios. This commonality can be attributed to the negative LMPs that are observed at bus #155 for all representative days. Furthermore, bus #155 is electrically close to bus #151, which is the connection point for 600 MW of wind generation and 191 MW of biomass generation. For the medium and low capital cost scenarios, the common storage locations are buses #90, #148, and #150. Bus #90 is electrically close to 690 MW of wind generation split between two wind farms at buses #148 and #150, which are connected through one or two lines to bus #155. Storage is installed at buses #149, #239, and #240 only for the low capital cost case. The installation at bus #149 is motivated by its proximity to bus #155, while buses #239 and #240 are close to 620 MW of wind generation and 118 MW of geothermal generation. Even under the least expensive capital cost scenario, storage is only installed at 7 out of 240 buses, thus suggesting that even in a system with significant renewable generation, there is only a relatively small number of locations where merchant storage can fully recover its investment cost.

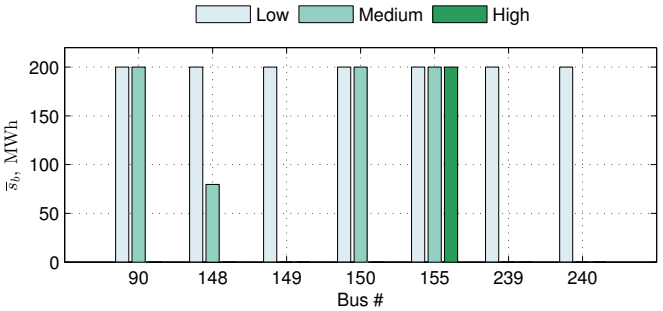

Fig. 3. Merchant storage siting and sizing without transmission expansion for the high, medium, and low capital cost scenarios.

[2]As in [14]–[16], the energy storage capital cost scenarios are itemized for the energy and power ratings. These itemized quantities can be aggregated in one parameter for a given value of ρ. For example, if $\rho = 5$ h, the total per kWh capital costs are $120/kWh, $250/kWh, and $335/kWh for the low, medium, and high capital cost scenarios. In terms of the power ratings, the low, medium, and high capital cost scenarios are $600/kW, $1,250/kW, and $1,675/kW. The range of these capital cost scenarios is consistent with the current and target capital costs for battery energy storage technologies [48].

This article has been accepted for publication in a future issue of this journal, but has not been fully edited. Content may change prior to final publication. Citation information: DOI 10.1109/TPWRS.2017.2705187, IEEE Transactions on Power Systems

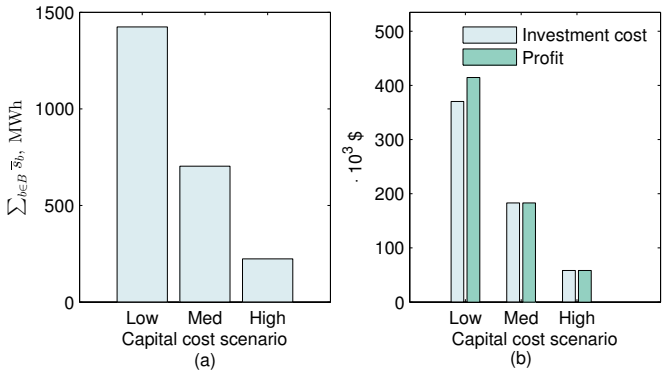

Fig. 4. Effect of the storage capital cost scenarios on storage investments: (a) total energy rating of storage; and (b) storage investment cost and lifetime profit.

The sizing decisions in Fig. 3 are constrained by the 200 MWh limit per bus, for all optimal locations and for all capital cost scenarios, except for bus #148 in the medium capital cost scenario. This observation suggests that spatial constraints on the most profitable locations could be a serious obstacle for the integration of storage. Fig. 4(a) shows the total energy rating of installed storage. Similar to the siting decisions, the total capacity of storage added is clearly affected by its capital cost. As one would expect, the lower capital cost, the more storage is installed. Under the low capital cost scenario, 1.4 GWh of storage is installed, which is about 3% of the peak hourly renewable production and about 1% of the peak hourly demand. Fig. 4(b) shows that, as the total energy rating of storage decreases with higher capital costs, so do the investment cost and storage lifetime profit. For the medium and high capital cost scenarios, the profit constraint is binding, i.e. the investment cost and lifetime profit are equal in Fig. 4(b). On the other hand, for the low capital cost scenario, the lifetime profit exceeds the investment cost by 11.2%. This difference indicates that storage owners may pursue higher rates of return as the capital cost of storage decreases.

The effect of varying the rate of return χ on the storage investment for the low capital cost scenario is illustrated in Fig. 5. Fig. 5(a) displays the status of the profit constraint by comparing the minimum rate of return χ with the actual χ^*, which is shown in Fig. 5(b). If $\chi^* > \chi$, the profit constraint is not binding, which is observed for $\chi \leq 1.15$. If $\chi > 1.15$, the profit constraint is binding, i.e. $\chi^* = \chi$, thus indicating that achieving higher rates of return is more challenging and requires more selective decisions on energy storage installation and leads to lower installed storage capacity, as shown in Fig. 5(c).

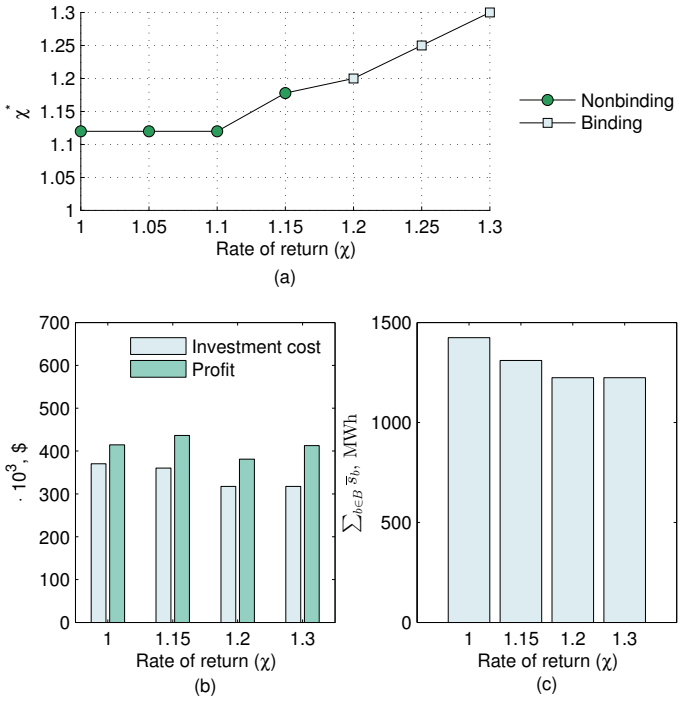

Fig. 5. Effect of the minimum rate of return χ on storage investments under the low capital cost scenario: (a) status of the profit constraint, where χ^* is the rate of return calculated using the outputs of the TL formulation; (b) storage investment cost and lifetime profit; and (c) total energy rating of storage.

C. Joint Merchant Storage and Transmission Expansion

The effect of transmission expansion decisions on storage investments is analyzed in two cases:

- **Case I**: The set of candidate lines for upgrades is limited to the lines directly connected to the buses where storage was located in Section IV-B (see Fig. 3).
- **Case II**: All transmission lines are considered for upgrade.

Table II itemizes the storage and transmission expansion decisions. In both cases, transmission expansion reduces the number and total installed storage capacity. However, the magnitude of this reduction depends on the capital cost of storage. When the capital cost is high, line #431 is upgraded in Case I and, because it is connected to bus #155, this decision prevents merchant storage from fully recovering its investment cost and, thus, no storage is installed. On the other hand, three lines are upgraded for the same cost scenario in Case II: line #432 (connected to bus #155), and lines #312 and #328, which are connected to buses with no storage and are congested due to a number of local thermal generators. Similarly, the transmission expansion decisions in Case II eliminate profit opportunities for merchant storage. However, as the capital cost of storage decreases, investments in both transmission and storage are made in both cases: storage is installed at some buses from the case without transmission expansion (#90, #155, #239), but also at new locations (#226, #227), which feature 236 MW and 2,144 MW of wind and hydro power generation. In Case I and Case II, the transmission expansion decisions are the same for the medium and low capital cost scenario. Compared to the high capital cost scenario, the decision to install storage changes with lines that should be upgraded and reduces the total added line capacity. Thus, the more affordable storage becomes, the less transmission expansion is needed. Compared to the case without transmission expansion, transmission expansion decisions under the low capital cost scenario reduce the total penetration of storage in Case I and Case II to 1.6% (0.74 GWh) and 1.2% (0.30 GWh) of the peak hourly renewable production.

This article has been accepted for publication in a future issue of this journal, but has not been fully edited. Content may change prior to final publication. Citation information: DOI 10.1109/TPWRS.2017.2705187, IEEE Transactions on Power Systems

TABLE II. COMPARISON OF MERCHANT STORAGE SITING AND SIZING WITHOUT AND WITH TRANSMISSION EXPANSION

Storage capital cost	No transmission expansion					Case I					Case II				
	Upgraded lines			Installed storage		Upgraded lines			Installed storage		Upgraded lines			Installed storage	
	Line #	Length (miles)	ΔF_l (MW)	Bus #	$\overline{s}_b$ (MWh)	Line #	Length (miles)	ΔF_l (MW)	Bus #	$\overline{s}_b$ (MWh)	Line #	Length (miles)	ΔF_l (MW)	Bus #	$\overline{s}_b$ (MWh)
Low	—	—	—	90 148 149 150 155 239 240	200 200 200 200 200 200 200	416	34.6	840	90 155 227 239	200 200 143.2 200	312 432	20.2 49.8	2000 1120	90 155 227	200 200 40.1
Medium	—	—	—	90 148 150 155	200 79.6 200 200	416	34.6	840	155 226 227	200 33.2 64.5	312 432	20.2 49.8	2000 1120	155 226 227	200 10.2 41.9
High	—	—	—	155	200	431	49.8	2667	—	—	312 328 432	20.2 120.3 49.8	2000 1800 1120	—	—

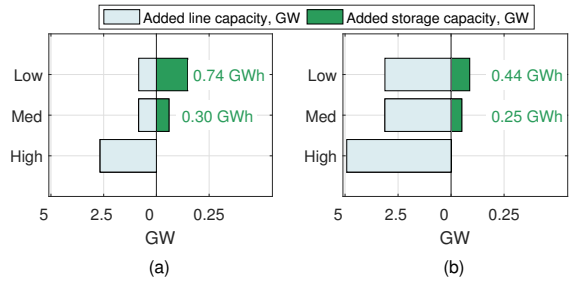

Fig. 6. Comparison of the total added transmission and storage power capacities (MW) for different capital cost scenarios: (a) Case I; and (b) Case II. The green numbers give the corresponding storage energy capacity (MWh). For comparison, in the no transmission expansion case the total added storage power (energy) capacities are 0.28 GW (1.4 GWh), 0.14 GW (0.68 GWh), 0.04 GW (0.2 GWh) for the low, medium, and high capital cost scenario.

Figure 6 compares the total added transmission and storage capacity in Case I and Case II for different storage capital cost scenarios. As expected, the total added storage capacity is sensitive to the capital cost and increases when the added transmission capacity decreases. Table III shows that transmission expansion reduces the lifetime profit expectations moderately in all the cases considered. However, the magnitude of this profit reduction decreases with the storage capital cost, suggesting that a lower capital cost makes storage decisions more robust to potential transmission expansion. Comparison between the profit reductions in Case I and Case II suggests that storage profits are more affected by the expansion of lines directly connected to the bus where storage is installed.

The expansion decisions on storage and transmission lines presented above are obtained assuming that no more than 200 MWh of storage can be placed at each bus. This limit is needed because of space and safety restrictions and may affect expansion decisions [15]. Therefore, the Case II experiments were repeated with different limits on the storage capacity that can be placed at every bus. For limits in the range from 100 MWh to 500 MWh of storage capacity per bus, transmission expansion decisions do not change, i.e. the same lines are chosen for upgrade as in Case II of Table II. On the other hand, Table IV shows that it does change the optimal

TABLE III. REDUCTION OF THE PROFITABILITY OF MERCHANT STORAGE COMPARED TO THE CASE WITHOUT TRANSMISSION EXPANSION (%)

Cost of storage	Case I	Case II
Low	2.41	2.76
Medium	2.76	2.81
High	3.13	3.34

TABLE IV. MERCHANT ENERGY STORAGE SITING AND SIZING DECISIONS FOR DIFFERENT ENERGY CAPACITY LIMITS AT EACH BUS

Cost of storage	Bus #	Energy capacity limit at each bus, MWh				
		100	200	300	400	500
Low	90	100.0*	200.0	100.0	11.1	12.0
	140	100.0*	–	–	–	–
	149	100.0	–	–	–	–
	155	100.0	200.0	300.0	364.8	366.1
	227	40.1	40.1	40.1	40.1	39.9
Medium	151	100.0	–	–	–	–
	155	100.0	200.0	232.0	231.8	231.7
	226	10.8	10.2	10.2	10.2	10.2
	227	40.6	41.9	41.7	41.6	41.6
High	–	–	–	–	–	–

* denotes that the number is rounded

expansion decisions on storage. Under the low and medium capital cost scenarios, as the value of the energy capacity limit increases, storage devices tend to be placed around bus #155, which is most advantageous for merchant operations. On the other hand, as the limit decreases and less storage capacity can be placed at that bus, the amount is distributed across buses that are in electrical proximity to bus #155. This effect of the energy capacity limit for merchant storage at each bus is similar to the effect of this limit on storage siting and sizing in a vertically-integrated environment as reported in [15]. As anticipated and similarly to the results of Table II, no storage is installed under the high capital cost scenario.

D. System Perspective

Table V shows that, as expected, investments in merchant storage lead to system-wide operating cost savings and reduced spillage of renewable generation. Both the operating cost savings and the spillage reductions increase monotonically for every case of transmission expansion as the storage capital

This article has been accepted for publication in a future issue of this journal, but has not been fully edited. Content may change prior to final publication. Citation information: DOI 10.1109/TPWRS.2017.2705187, IEEE Transactions on Power Systems

TABLE V. OPERATING COST SAVINGS AND SPILLAGE REDUCTIONS FOR DIFFERENT CAPITAL COST SCENARIOS COMPARED TO THE CASE WITHOUT STORAGE AND TRANSMISSION EXPANSION (%)

Parameter	Cost of storage	No trans. expansion	Case I	Case II
Operating cost savings	Low	3.04	4.63	6.88
	Medium	2.74	3.18	4.06
	High	0.46	0.71	1.37
Spillage reduction	Low	7.09	7.76	6.93
	Medium	3.17	5.04	2.56
	High	4.75	4.92	1.87

cost reduces. Cases I and II offer greater operating cost savings than the case without transmission expansion, thus emphasizing the value to the system of co-planning transmission and merchant storage expansion. Spillage of renewable generation decreases in Case I relative to the case without transmission expansion, but increases in Case II. This can be explained by the fact that the proposed model does not explicitly minimize spillage and opts alternative dispatch decisions. Further investigation is required to quantify additional system-wide operating cost savings that can be attained if merchant energy storage can simultaneously participate in other markets.

E. Computational Performance

Since the solution technique described in Section III has previously been scrutinized in [32], [38], the scope of this section is limited to the computational performance of the proposed TL model. All simulations presented in this case study were completed within 72 hours and 7 iterations. The average computing time in Case II of Section IV-C, the most computationally demanding experiment in this paper, was 12.6 hours and took 4 iterations (rounded). Our numerical experiments also suggest that the computational performance is most sensitive to parameter $N_{\hat{L}}$, the maximum number of candidate lines for expansion, as shown in Fig. 7. As the number of candidate lines increases, so does the computing time. This increase mainly occurs due to the SP and can be attributed to the increase in binary combinations to be considered due to (13).

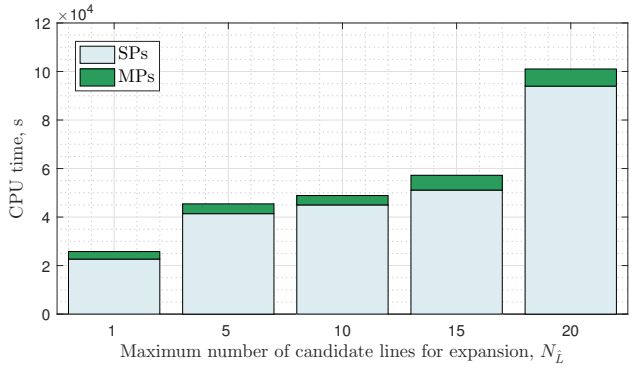

Fig. 7. Solution time for different values of the maximum number of candidate lines for expansion ($N_{\hat{L}}$). Label 'MPs' and 'SPs' denote the total solution times of all master problems and subproblems during all iterations.

V. CONCLUSION

This paper describes a tri-level model and a solution technique for joint planning of transmission expansion and merchant storage in a market-based power system. A realistic 240-bus, 448-line model of the WECC system demonstrates that investing in merchant storage is economically justified for all three capital cost scenarios considered. However, even under the low capital cost and without transmission expansion, only 7 out of 240 buses have sufficient profit opportunities for merchant storage. In this case, the optimal storage penetration is estimated at 3% of the peak hourly renewable production. A qualitative analysis of the optimal locations suggests that the most profitable locations are in proximity of renewable generation facilities (primarily wind), congested lines, and bulk conventional generation. However, potential transmission expansion may eliminate some of the profit opportunities and reduce storage penetration to 1.2% of the peak hourly renewable production. From a system perspective, co-planning of storage and transmission expansion achieves greater operating cost savings than solely the deployment of storage.

Some limitations of the proposed model indicate the following directions for future work:

- The proposed model can be modified to account for additional profits that merchant storage can attain by participating in other than a day-ahead electricity market (e.g., capacity markets, ancillary services [53], hour-ahead). These profit streams may improve profitability of merchant energy storage.
- The proposed model is developed for existing market rules that are likely to change in order to accommodate higher penetrations of renewable generation (e.g. carbon emission limits or taxes). These changes may affect profitability of merchant storage.
- There is a need to incorporate subhourly timescales to adequately capture real-time storage dynamics and effects of real-time price volatility on the lifetime storage profitability.
- The proposed model assumes that future technical parameters of energy storage ($\aleph^{\mathrm{c}}, \aleph^{\mathrm{d}}, \rho$) and their capital cost scenarios are known with perfect accuracy. In practice, these parameters are uncertain and may significantly affect the profitability of merchant energy storage and its value to the system. There is a need to consider this uncertainty in the proposed model and account for its distribution during the planning horizon.

REFERENCES

[1] A. Castillo and D. F. Gayme, "Grid-scale energy storage applications in renewable energy integration: A survey", *En. Conv. and Manag.*, Vol. 87, pp. 885-894, Nov. 2014.

[2] H. Mohsenian-Rad, "Coordinated price-maker operation of large energy storage units in nodal energy markets," *IEEE Trans. Power System*, vol. 31, no. 1, pp. 786-/797, Jan. 2016.

[3] J. H. Roh, M. Shahidehpour, and L. Wu, "Market-based generation and transmission planning with uncertainties," *IEEE Trans. Power Syst.*, vol. 24, no. 3, pp. 1587-1598, Aug. 2009.

[4] J. Shan and S.M. Ryan, "A tri-level model of centralized transmission and decentralized generation expansion planning for an electricity market—Part I," *IEEE Trans. Power System*, vol. 29, no. 1, pp. 132–141, Jan. 2014.

[5] F. D. Munoz, B. F. Hobbs, J. L. Ho, and S. Kasina, "An engineering-economic approach to transmission planning under market and regulatory uncertainties: WECC case study," *IEEE Trans. Power System*, vol. 29, no. 1, pp. 307–317, Jan. 2014.

[6] W. Qi, Y. Liang, and Z.-J. M. Shen, "Joint planning of energy storage and transmission for wind energy generation," *Op. Res.*, vol. 63, no. 6, pp. 1280–1293, Dec. 2015.

[7] I. Konstantelos and G. Strbac, "Valuation of flexible transmission investment options under uncertainty," *IEEE Trans. Power System*, vol. 30, no. 2, pp. 1047–1055, March 2015.

[8] T. Qiu, B. Xu, Y. Wang, Y. Dvorkin, and D. S. Kirschen, "Stochastic Multi-stage co-planning of transmission expansion and energy storage," *IEEE Trans. Power System*, vol. 32, no. 1, pp. 643–651, Jan. 2017.

[9] M. Hedayati, J. Zhang, and K. W. Hedman, "Joint transmission expansion planning and energy storage placement in smart grid towards efficient integration of renewable energy," in *Proc. of the 2014 IEEE PES T&D Conf. and Exp.*, pp. 1–5, Chicago, IL, USA, 2014.

[10] R. Go, F.D. Munoz, and J. P. Watson, "Assessing the economic value of co-optimized grid-scale energy storage investments in supporting high renewable portfolio standards," *Applied Energy*, vol. 183, pp. 902–913, 2016.

[11] V. Krishnan and T. Das, "Optimal allocation of energy storage in a co-optimized electricity market: Benefits assessment and deriving indicators for economic storage ventures," *Energy*, vol. 81, pp. 175–188, Mar. 2015.

[12] B. Xu, Y. Wang, Y. Dvorkin, R. Fernandez-Blanco, C. A. Silva-Monroy, J. P. Watson, anf D. S. Kirschen, "Scalable Planning for Energy Storage in Energy and Reserve Markets," *IEEE Transactions on Power Systems*, early access, 2017.

[13] E. Nasrolahpour, H. Zareipour, W. D. Rosehart and S. J. Kazempour, "Bidding strategy for an energy storage facility," in Proc. of the *2016 Power Systems Computation Conference (PSCC)*, Genoa, Italy, 2016, pp. 1–7.

[14] Y. Dvorkin, R. Fernández-Blanco, D. S. Kirschen, H. Pandžić, J.-P. Watson, and C. A. Silva-Monroy, "Ensuring profitability of energy storage," *IEEE Trans. Power System*, vol. 32, no. 1, pp. 611–623, Jan. 2017.

[15] R. Fernández-Blanco, Y. Dvorkin, B. Xu, Y. Wang, and D. S. Kirschen, "Optimal energy storage siting and sizing: A WECC case study,"' *IEEE Trans. Sust. En.*, early access, 2017.

[16] H. Pandžić, Y. Wang, T. Qiu, Y. Dvorkin, and D. S. Kirschen, "Near-optimal method for siting and sizing of distributed storage in a transmission network," *IEEE Trans. Power System*, vol. 30, no. 5, pp. 2288–2300, Sep. 2015.

[17] S. Wogrin and D. F. Gayme, "Optimizing storage siting, sizing, and technology portfolios in transmission-constrained networks," *IEEE Trans. Power System*, vol. 30, no. 6, pp. 3304–3313, Nov. 2015.

[18] K. Dvijotham, M. Chertkov, and S. Backhaus, "Storage sizing and placement through operational and uncertainty-aware simulations," in Proceedings of the *47th HI Int. Conf. on Syst. Sc.*, pp. 2408–2416, 2014.

[19] D. Pudjianto, M. Aunedi, P. Djapic, and G. Strbac, "Whole-systems assessment of the value of energy storage in low-carbon electricity systems," *IEEE Trans. Smart Grid*, vol. 5, no. 2, pp. 1098–1109, Mar. 2014.

[20] A. Castillo and D. F. Gayme, "Profit maximizing storage allocation in power grids," in Proc. of the *2013 IEEE 52nd Annual Conf. on Dec. and Contr.l*, pp. 429–435, Dec. 2013.

[21] H. Pandžić and I. Kuzle, "Energy storage operation in the day-ahead electricity market," in Proc. of the 2015 12th Int. Conf. on the Eur. En. Mkt, pp. 1–6, May 2015.

[22] Y. Wang, Y. Dvorkin, R. Fernandez-Blanco, B. Xu, T. Qiu, and D. Kirschen, "Look-Ahead Bidding Strategy for Energy Storage," *IEEE Transactions on Sustainable Energy*, early access, 2017.

[23] E. Nasrolahpour, S. J. Kazempour, H. Zareipour, and W. D. Rosehart, "Strategic sizing of energy storage facilities in electricity markets," *IEEE Trans. Sust. En.*, vol. 7, no. 4, pp. 1462–1472, Oct. 2016.

[24] S. de la Torre, A. J. Conejo and J. Contreras, "Transmission expansion planning in electricity markets," *IEEE Trans. Power System*, vol. 23, no. 1, pp. 238–248, Feb. 2008.

[25] L. Baringo and A. J. Conejo, "Transmission and wind power investment," *IEEE Trans. Power System*, vol. 27, no. 2, pp. 885–893, May 2012.

[26] Y. Dvorkin, D. S. Kirschen and M. A. Ortega-Vazquez, "Assessing flexibility requirements in power systems," *IET Generation, Transmission & Distribution*, vol. 8, no. 11, pp. 1820-1830, 11 2014.

[27] Y. Dvorkin, M. Lubin, S. Backhaus and M. Chertkov, "Uncertainty sets for wind power generation," *IEEE Transactions on Power Systems*, vol. 31, no. 4, pp. 3326-3327, July 2016.

[28] D. Kirschen and G. Strbac, *Fundamentals of Power System Economics*. Chichester, UK: John Wiley & Sons, Ltd, 2004.

[29] P. Donohoo, "Design of wide-area electric transmission networks under uncertainty: methods for dimensionality reduction," *Ph.D. Thesis*, *MIT*, USA, 2013. [Online]. Available at: http://goo.gl/G7U7df.

[30] S. Wogrin, E. Centeno, and Julian Barquin, "Generation capacity expansion analysis: Open loop approximation of closed loop equilibria," *IEEE Trans. Power System*, vol. 28, pp. 3362–3371, 2013.

[31] Western Electricity Coordinating Council, TEPPC Transmission Planning Protocol, Technical Report, 2012. [Online]. Available at: https://www.wecc.biz/Corporate/TEPPC_PlanningProtocol.pdf

[32] C. Ruiz and A. J. Conejo, "Robust transmission expansion planning," *Eur. J. of Op. Res.*, vol. 242, pp. 390-401, 2015.

[33] R. Domínguez, A. J. Conejo, and M. Carrión, "Toward fully renewable electric energy systems," *IEEE Trans. Power Syst.*, vol. 30, pp. 316–326, 2015.

[34] J. A. Taylor, S. V. Dhople, and D. S. Callaway, "Power systems without fuel," *Renew. and Sust. En. Rev.*, vol. 57, Jun. 2016.

[35] Z. Hu, F. Zhang, and B. Li, "Transmission expansion planning considering the deployment of energy storage systems," in Proc. of the *2012 IEEE Power and Energy Society General Meeting*, San Diego, California, July 2012.

[36] J. M. Arroyo, "Bilevel programming applied to power system vulnerability analysis under multiple contingencies," *IET Gen., Trans. & Distr.*, vol. 4, pp. 178–190, 2010.

[37] R. Fernández-Blanco, J. M. Arroyo, and N. Alguacil, "Bilevel programming for price-based electricity auctions: A revenue-constrained case, EURO Journal on Computational Optimization, vol. 3, no. 3, pp. 163–195, Sep. 2015.

[38] B. Zeng and L. Zhao, "Solving two-stage robust optimization problems using acolumn-and-constraint generation method," *Op. Res. Let.*, vol. 41, no. 5, 2013, pp. 457–461.

[39] C. A. Floudas, *Nonlinear and Mixed-Integer Optimization: Fundamentals and Applications*. New York, NY, USA: Oxford Univ. Press, 1995.

[40] S. J. Kazempour and A. J. Conejo, "Strategic generation investment under uncertainty via Benders decomposition," *IEEE Trans. Power System*, vol. 27, pp. 424–432, 2012.

[41] L. Baringo and A. J. Conejo, "Wind power investment: A Benders decomposition approach," *IEEE Trans. Power System*, vol. 27, pp. 433–441, 2012.

[42] J. E. Price and J. Goodin, "Reduced network modeling of WECC as a Market Design Prototype," in *Proc. of the 2011 IEEE Pwr. and En. Soc. Gen. Meet.*, 2011, pp. 1–5.

[43] Western Electricity Coordinating Council, "TEPPC Study Report 2024 PC1 Common Case," *Technical report*, 2015. [Online]. Available at: https://www.wecc.biz/Administrative/150805_2024%20CCV1.5_StudyReport_draft.pdf

[44] B. Pitt, "Applications of data mining techniques to electric load profiling", *PhD thesis*, Un. of Manch., UK, 2000. [Online]. Available at: http://goo.gl/atUigh

[45] K. Poncelet, H. Hoschle, E. Delarue, A. Virag, and W. D. haeseleer, "Selecting representative days for capturing the implications of integrating intermittent renewables in generation expansion planning problems," *IEEE Trans. Power System*, early access, 2016.

[46] K. Poncelet, E. Delarue, D. Six, J. Duerinck, and W. Dhaeseleer, "Impact of the level of temporal and operational detail in energy-system planning models," *Applied Energy*, vol. 162, pp. 631–643, 2016.

[47] P. Nahmmacherand, E. Schmid, L. Hirth, and B. Knopf, "Carpe Diem: A novel approach to select representative days for long-term power system models with high shares of renewable energy sources", United States Association for Energy Economics Working Paper No. 14–194, 2014. [Online]. Available at: http://ssrn.com/abstract=2537072.

[48] U.S. Department of Energy, "Grid energy storage," Technical report, Dec. 2013. [Online]. Available at: http://www.sandia.gov/ess/docs/other/Grid_Energy_Storage_Dec_2013.pdf

[49] "Capital Costs for Transmission and Substations. Updated Recommendations for WECC Transmission Expansion Planning," WECC, 2014. [Online]. Available at: https://goo.gl/QHoMKH

[50] Hyak Supercomputer, 2016. [Online]. Available at: http://goo.gl/IBEOoS

[51] The IBM ILOG CPLEX website, 2016. [Online]. Available at: http://goo.gl/Zr8OEW

[52] R. E. Rosenthal, "GAMS – A Users Guide", GAMS Corp., 2013. [Online]. Available at: http://goo.gl/gokQxs

[53] Bolun Xu, Y. Dvorkin, D. S. Kirschen, C. A. Silva-Monroy and J. P. Watson, "A comparison of policies on the participation of storage in U.S. frequency regulation markets," in Proc. of the *2016 IEEE Power and Energy Society General Meeting*, Boston, MA, 2016, pp. 1-5.

Yury Dvorkin (S'11-M'16) received his Ph.D. degree from the University of Washington, Seattle, WA, USA, in 2016.

Dvorkin is currently an Assistant Professor in the Department of Electrical and Computer Engineering at New York University, New York, NY, USA. Dvorkin was awarded the 2016 Scientific Achievement Award by Clean Energy Institute (University of Washington) for his doctoral dissertation "Operations and Planning in Sustainable Power Systems". His research interests include short- and long-term planning in power systems with renewable generation and power system economics.

Ricardo Fernández-Blanco (S'10-M'15) received the Ingeniero Industrial degree and the Ph.D. degree in electrical engineering from the Universidad de Castilla-La Mancha, Ciudad Real, Spain, in 2009 and 2014, respectively.

He is currently a Scientific/Technical Project Officer at the JRC.C7 Knowledge for the Energy Union (Joint Research Center), Petten, The Netherlands. His research interests include the fields of operations and economics of power systems, bilevel programming, hydrothermal coordination, and electricity markets.

Yishen Wang (S'12) received the B.S. degree from the Department of Electrical Engineering, Tsinghua University, Beijing, China, in 2011. He is currently pursuing the Ph.D. degree in electrical engineering at the University of Washington, Seattle, WA, USA.

His research interests include power system economics and operation, energy storage, renewable forecasting and electricity markets.

Bolun Xu (S'14) received B.S. degrees in Electrical and Computer Engineering from the University of Michigan, Ann Arbor, USA and Shanghai Jiaotong University, Shanghai, China in 2011, and the M.Sc degree in Electrical Engineering from Swiss Federal Institute of Technology, Zurich, Switzerland in 2014.

He is currently pursuing the Ph.D. degree in Electrical Engineering at the University of Washington, Seattle, WA, USA. His research interests include energy storages, power system operations, and power system economics.

Daniel S. Kirschen (M'86-SM'91-F'07) received the degree in electrical and mechanical engineering from the Universite Libre de Bruxelles, Brussels, Belgium, and the M.Sc. and Ph.D. degrees from the University of Wisconsin, Madison, WI, USA, 1979, 1980, and 1985, respectively.

He is currently a Close Professor of Electrical Engineering with the University of Washington, Seattle, WA, USA. His research interests include smart grids, the integration of renewable energy sources in the grid, power system economics, and power system security.

Hrvoje Pandžić (S'06-M'12) received the M.E.E. and Ph.D. degrees from the Faculty of Electrical Engineering and Computing, University of Zagreb, Zagreb, Croatia, in 2007 and 2011, respectively. From 2012 to 2014, he was a Postdoctoral Researcher with the University of Washington, Seattle, WA, USA.

Currently, he is an Assistant Professor with the Faculty of Electrical Engineering and Computing, University of Zagreb. His research interests include planning, operation, control, and economics of power and energy systems.

Jean-Paul Watson (M'10) received the B.S., M.S., and Ph.D. degrees in computer science.

He is a Distinguished Member of Technical Staff with the Discrete Math and Optimization Department, Sandia National Laboratories, Albuquerque, NM, USA. He leads a number of research efforts related to stochastic optimization, ranging from fundamental algorithm research and development, to applications including power grid operations and planning.

Cesar A. Silva-Monroy (M'15) received the B.S. degree from the Universidad Industrial de Santander, Bucaramanga, Colombia, and the M.S. and Ph.D. degrees from University of Washington, Seattle, WA, USA, all in electrical engineering.

He is a Senior Member of Technical Staff with Sandia National Laboratories, Albuquerque, NM, USA. He currently leads projects on electric grid resilience, planning and operations. His research interests also include electricity markets and renewable energy integration